AIP | The Journal of Chemical Physics

Small periodic cluster calculation on point defect problems in hexagonal layered solids

Alex Zunger

Citation: The Journal of Chemical Physics **62**, 1861 (1975); doi: 10.1063/1.430670
View online: http://dx.doi.org/10.1063/1.430670
View Table of Contents: http://scitation.aip.org/content/aip/journal/jcp/62/5?ver=pdfcov
Published by the AIP Publishing

Small periodic cluster calculation on point defect problems in hexagonal layered solids

Alex Zunger

Department of Chemistry, Tel Aviv University, Tel Aviv, Israel

Department of Theoretical Physics, Soreq Nuclear Research Centre, Yavne, Israel
(Received 25 March 1974)

A model is proposed for discussing deep defect levels in covalent solids, based on the representation of the one-electron energies of the crystal by the eigenvalue spectrum of a small periodic cluster of atoms. Calculations of this model by semiempirical MO–LCAO methods for a vacancy problem in hexagonal boron nitride and graphite and substitutional boron impurity in graphite, yield satisfactory results when compared with experimental EPR, thermoluminescence, and thermally-stimulated-currents data.

I. INTRODUCTION

The problem of describing the electronic states of defects in semiconducting and insulating covalent solids has usually been treated either by the infinite perfect crystal band states that satisfy translational invariance[1–3] or by the "defect molecule" approach that constructs the defect states from its local environment.[4,5] While the former approach does not provide a way of introducing lattice relaxations around the defect site and has supplied only limited information regarding the charge distribution due to the defect states, the highly localized approach does not describe the location of these states relative to the band edges. An intermediate approach, adopted recently by Messmer and Watkins,[6] Larkins,[7] and Zunger[8] treated the deep defect problem by considering a large cluster of host atoms containing the defect and seeking the convergence limit of its one-electron energy states, formulated by LCAO molecular orbital theory, as a function of cluster size. For relatively large clusters, this yields the approximate location of the defect levels relative to the band edges and also provides a simple means for calculating the charge distribution of the defect orbitals and introducing lattice relaxations around it. However, the main disadvantages of this approach are as follows: (i) The boundary conditions employed for the finite cluster (usually hydrogen atoms satisfying the valence of the dangling bonds on the surface) result in unrealistic charge inhomogeneity over the cluster,[7–9] making the calculation of properties that are sensitive to charge distribution questionable. Relaxation of these boundary conditions[7,9] results in somewhat drastic effects on the location of the band edges and on the band width. (ii) The one-electron energy levels deduced from molecular cluster models for the ideal clusters do not exhibit a simple correspondence to energies in the Brillouin zone (B. Z.) of the infinite crystal[6,7] unless special symmetries are considered.[9] Band structure calculations for infinite periodic crystals, employing the same LCAO approach,[6,9] yield results that differ significantly from those of the finite cluster calculations.

We wish to present a model for the electronic levels in the solid by which it will be possible to treat both the electronic band structures of the ideal lattice and point defect levels, on the same level of approximation, thereby providing a correlative scheme between the band and defect levels. We also demand that it will be possible to treat within the suggested model small distortions around the defect site and that the atomic charge distribution in the defect level will be amenable to simple calculation. We start by considering the ideal lattice states.

II. CRYSTAL ORBITAL APPROACH

A common crystal orbital scheme consists of representing a crystal one-electron energy function as a combination of Bloch functions $\Phi_\mu(\tilde{K})$, where μ denotes the different atomic representations (sublattice sites and atomic orbitals). The Bloch function is taken as a combination of atomic orbitals $\chi_\mu(\tilde{r}-\tilde{R}_l)$ centered on the atom in position R_l:

$$\Phi_\mu(\tilde{K}) = M^{-1/2}\sum_{l=1}^{N} e^{i\tilde{K}\cdot\tilde{R}_l}\chi_\mu(\tilde{r}-\tilde{R}_l)\ , \qquad (1)$$

where N is the number of unit cells and $\mu = 1, 2, \ldots, \sigma$. The matrix elements of the Hartree–Fock one-electron operator $\hat{F}$ between different Bloch states are given by

$$F_{\mu\lambda}(\tilde{K}) = \sum_{n=1}^{N} e^{i\tilde{K}\cdot\tilde{R}_n}\langle\chi_\mu(\tilde{r})\,|\hat{F}|\,\chi_\lambda(\tilde{r}-\tilde{R}_n)\rangle\ , \qquad (2)$$

where the first atom was taken to be at the origin. The overlap integral between Bloch states is likewise given by

$$S_{\mu\lambda}(\tilde{K}) = \sum_{n=1}^{N} e^{i\tilde{K}\cdot\tilde{R}_n}\langle\chi_\mu(\tilde{r})\,|\,\chi_\lambda(\tilde{r}-\tilde{R}_n)\rangle\ . \qquad (3)$$

The eigenvalue problem arrived at by applying the variation principle is defined by the simultaneous set of σ equations for the coefficients $C_{i\lambda}(\tilde{K})$; $i, \lambda = 1, 2, \ldots, \sigma$ and band energies $E_i(\tilde{K})$:

$$\sum_{\lambda=1}^{\sigma}[F_{\mu\lambda}(\tilde{K}) - S_{\mu\lambda}(\tilde{K})E_i(\tilde{K})]C_{i\lambda}(\tilde{K}) = 0\ , \qquad (4)$$

where $C_{i\lambda}(\tilde{K})$ are the expansion coefficients of the crystal orbital in terms of the atomic basis set and $i = 1, 2, \ldots, \sigma$. It is important to note that the Hartree–Fock operator $\hat{F}$ is determined by the charge density contributed by *all* electrons and is therefore dependent on the complete set of solutions $\{C_{i\lambda}(\tilde{K})\}$ where $\tilde{K}$ are the vectors spanning the entire Brillouin zone. The solution of Eq. (4) for a particular $\tilde{K}_n$ value therefore involves the knowledge of the bond-charge matrix of n_{occ} occupied levels, which determines $F_{\mu\lambda}(\tilde{K})$:

$$P_{\lambda\lambda'}(\tilde{K}) = \sum_{i=1}^{n_{\text{occ}}} C^*_{i\lambda}(\tilde{K}) C_{i\lambda'}(\tilde{K}) \tag{5}$$

for the entire B.Z. and therefore the solutions $\{C_{i\lambda}(\tilde{K})\}$ have to be determined self-consistently.

In conventional tight-binding (TB) approximation, the self-consistent coupling between various wave vectors via the matrix elements appearing in Eq. (2) is neglected and the latter equation is replaced by the perturbative expression

$$F_{\mu\lambda}(\tilde{K}) = \sum_{n=1}^{N} e^{i\tilde{K}\cdot\tilde{R}_n} \langle \chi_\mu(\tilde{r}) \,|\, V(\tilde{r}-\tilde{R}_n) \,|\, \chi_\lambda(\tilde{r}-R_n) \rangle \ , \tag{6}$$

where $V(\tilde{r}-\tilde{R}_n)$ is the periodic potential, combined from free-atom (in covalent solids) or free-ion (in ionic and metallic solids) potentials. This approximation fails completely when the crystalline environment strongly changes the free-atom character of the potential at a given atomic site. These effects may occur in several systems, such as

(i) solids where strong ionic–covalent bonding occurs in the unit cell made up of atoms with different electronegativities (such as the binary III–V crystals). In this case, partial interatomic charge transfer strongly modifies the free-atom character of the potential around an atomic site.[9]

(ii) hydrogen-bonded systems which exhibit considerable charge redistribution in the solid relative to the neutral free constituents, as manifested by partial ionic character (solid HF, KH_2PO_4, etc.).

(iii) homopolar covalent solids (such as graphite), where the spherical character of the atomic constituents in their free form is modified in the crystal due to the lower symmetry at the atomic site.

It should also be mentioned that the construction of $V(\tilde{r}-\tilde{R}_n)$ from isolated-atom potentials for calculating point defects levels in covalent solids is similarly questionable when charge redistribution effects introduced by the defect site are considerable.

Non-self-consistent TB calculations employing computed matrix elements of free-atom potentials that have been performed on graphite[10,11] and boron nitride (BN)[12,13] yield poor agreement with experimental optical data and, therefore, a semiempirical approach was adopted. In this approach, either one scales the various matrix elements appearing in Eqs. (3) and (6) to yield best fit to some of the experimental data,[10,12] or one uses instead similar matrix elements appearing in molecular calculations that were already adjusted to reproduce the optical spectrum of related small molecules.[11,13] This approach is deductive in nature and depends on the availability of sufficient experimental data. In the case of BN and graphite, the experimental optical data mainly consists of π electron transitions and therefore the σ matrix elements remained arbitrarily scaled. Also, the scaling factors or the molecular matrix elements employed can be determined only for the experimental interatomic separation at normal pressure, and therefore the calculation of density-dependent properties such as equilibrium interatom separation and pressure dependence of various electronic properties is impossible without further input. The use of free-atom potentials in non-self-consistent calculations also neglects a large part of the $\sigma-\pi$ interactions in the above-mentioned solids. This might have a considerable effect on the $\sigma-\pi$ band overlapping and on the computed atomic charges.[9,11]

The self-consistent approach to the energy band calculation, based on the recompilation of the crystal potential on the basis of the calculated band structure, has been carried out only in recent years. Stukel *et al.*[14] presented a self-consistent APW calculation for binary sphalerite crystals; Rudge[15] applied the self-consistent approach to APW method; and Brust[16] suggested a self-consistent pseudopotential approach. Herman *et al.*[17] considered various combinations of first-principle and empirically adjusted OPW calculations, and Mattheiss *et al.*[18] have presented a charge-self-consistent APW approach for transition metal solids, in which the contribution to the charge density of all occupied states below the Fermi level is used for computing the crystal potential. Self-consistent tight-binding calculations have been performed on a group of organic polymers by Del-Re *et al.*,[19] Andre,[20] Imamuara,[21] Morakuma,[22] O'Shea and Santry,[23] and Beveridge and Jano,[24] and on hexagonal boron nitride by Zunger.[9] It has been shown that in binary crystals consisting of atoms from different rows in the periodic table, the iteration of the potential to self-consistency changes the band structure by the order of 1 eV up to several eV, as compared to the uniterated results. The self-consistent method yields stabilized band structure and enables the calculation of interatom-distance-dependent properties.[9,15] Its deficiency in the context discussed here lies in the fact that it relies heavily on the assumption of perfect periodicity of the lattice and is therefore not suitable for considering local perturbations in lattice periodicity such as defects, lattice relaxations, etc.

III. METHOD OF CALCULATION

We present here a different method, intermediate between the truncated crystal picture and the self-consistent band model, for treating both ideal crystal and defects levels, similar to the crystal orbital approach treated recently by Davidson and Levine.[25] Instead of explicitly using the translational symmetry of the lattice to reduce the original $\sigma N\times\sigma N$ matrix secular equations to $\sigma\times\sigma$ from Eq. (4), we now retain the $\sigma N\times\sigma N$ basis and use a crystal orbital that is a linear combination of σN atomic orbitals:

$$\psi_i = \sum_{\mu=1}^{\sigma} \sum_{n=0}^{N-1} C_{\mu n i}\chi_\mu(\tilde{r}-\tilde{R}_n) \ , \tag{7}$$

where $\mu = 1, \ldots, \sigma$ denotes the atomic orbitals and $n = 0, 1, \ldots, N-1$ numbers the atoms and i ranges from 1 to σN.

We require that the array of N atoms will form a "pseudomolecule" that is periodic in space, and is characterized by a range of interaction η. The range of interaction η is determined by the symmetry of the crystal and by N alone (e.g., a cluster of $N=2\eta+1$ atoms can be used to represent a one-dimensional chain in which each atom experiences η order of neighboring interactions). The secular equations are given by

$$\sum_{\mu,n}[F_{\mu n,\lambda m}-S_{\mu n,\lambda m}E_i]C_{\mu n i}=0\ , \tag{8}$$

and the matrix elements, expressed in the atomic basis set, are

$$\begin{aligned} F_{\mu n,\lambda m}&=\langle\chi_\mu(\tilde{r}-\tilde{R}_n)|\hat{F}|\chi_\lambda(\tilde{r}-\tilde{R}_m)\rangle\ , \\ S_{\mu n,\lambda m}&=\langle\chi_\mu(\tilde{r}-\tilde{R}_n)|\chi_\lambda(\tilde{r}-\tilde{R}_m)\rangle\ . \end{aligned} \tag{9}$$

Owing to the periodicity imposed on the finite cluster, the solutions E_i form a subset of the full eigenvalue spectrum of the infinite ($N\to\infty$) lattice. The operator $\hat{F}$ is now expressed in real space rather than in $\tilde{K}$ space, using the following form of the density matrix:

$$\begin{aligned} \rho(\tilde{r})&=\sum_{\mu n,\lambda m}P_{\mu n,\lambda m}\chi_\mu(\tilde{r}-\tilde{R}_n)\chi_\lambda(\tilde{r}-\hat{R}_m)\ , \\ P_{\mu n,\lambda m}&=2\sum_i^{n_{\rm occ}}C^*_{\mu n i}C_{\lambda m i}\ . \end{aligned} \tag{10}$$

It depends on the charge density contributed by all electrons in $n_{\rm occ}$ levels as in conventional LCAO–SCF formalism. Once the atomic basis set is defined (usually valence atomic orbitals are used, i.e., $=2s$, $2p_x$, $2p_y$, and $2p_z$ orbitals for second row atoms) and a method of calculating the matrix elements of $\hat{F}$ in atomic basis set (usually, as will be later noted, various levels of approximations are involved), the solution of Eq. (8) depends on the atomic positions in the cluster. Since the solutions $E_i\equiv E_{\lambda,n}$ are obviously invariant under rigid translations and rotations of the N atom cluster, it is sufficient to specify the interatom distance matrix $D^{(\eta)}_{pp'}$ and the interatom direction-cosine matrices $E^{(\eta)}_{pp'}(x)$, $E^{(\eta)}_{pp'}(y)$, and $E^{(\eta)}_{pp'}(z)$ (where p,p' number the atomic sites) relative to arbitrary x, y, z directions, in order to solve (8). The definition of the absolute coordinates of each atom with reference to a fixed origin is not required.

This freedom is used by requiring that the four matrices simultaneously fulfill the following two properties (that cannot be accomplished by the set of atomic coordinates):

(i) They represent a periodic N-atom cluster with interaction range $\eta(N)$.

(ii) The matrices are built according to the desired point symmetry of the investigated solid.

As an example, a seven-atom one-dimensional linear chain with an interatom distance a, and directed along an arbitrary axis x, has 3 orders of interactions, and is described by

$$D^{(3)}_{pp'}=\begin{pmatrix} 0&1&2&3&3&2&1\\ 1&0&1&2&3&3&2\\ 2&1&0&1&2&3&3\\ 3&2&1&0&1&2&3\\ 3&3&2&1&0&1&2\\ 2&3&3&2&1&0&1\\ 1&2&3&3&2&1&0 \end{pmatrix}\ ,$$

$$E^{(3)}_{pp'}(x)=\begin{pmatrix} 0&1&1&\cdots&\cdots&1\\ -1&0&1&\cdots&\cdots&1\\ -1&-1&0&1&\cdots&1\\ -1&-1&&&&\\ -1&&&&&0 \end{pmatrix}\ ,$$

while $E^{(3)}_{pp'}(y)$ and $E^{(3)}_{pp'}(z)$ are identically zero.

The problem is thus reduced to the solution of a fictitious N-atom molecule whose structure is given by the matrices $D^{(\eta)}_{pp'}$, $E^{(\eta)}_{pp'}(x)$, $E^{(\eta)}_{pp'}(y)$, and $E^{(\eta)}_{pp'}(z)$, by a LCAO–SCF one-electron method. Each atom on a given sublattice experiences an identical crystalline surrounding in such a pseudomolecule and a full account of charge redistribution effects is taken via the self-consistent solution of Eq. (8). The deficiencies of the non-self-consistent crystal orbital method [Eqs. (4) and (6)] previously mentioned are thus overcome. The resulting eigenvalues $E_{\lambda,n}$ can of course be classified, in the case of perfect periodicity, according to the wave vectors $\tilde{K}_n$; $n=0,\ldots,N-1$ by recognizing that

$$C_{\mu n j}=C_{\mu j}e^{i\tilde{K}_n\cdot\tilde{R}_n}\ \text{and}\ E_{\lambda,n}=E_\lambda(\tilde{K}_n)\ , \tag{11}$$

where $K_n=(2\pi/Na)n$.

The method of obtaining $E_\lambda(\tilde{K}_n)$ for a finite periodic cluster of N atoms is completely analogous to the self-consistent procedure outlined in Eqs. (1)–(5), provided that only the subset $\tilde{K}_n$; $n=0,\ldots,N-1$ is considered by the latter method. The values $E_\lambda(\tilde{K}_n)$ obtained by the former method converge to the limit of the appropriate band energies of the infinite lattice, obtained by the latter method, as the order of interaction $\eta(N)$ increases. Note that in the small periodic cluster (SPC) approach, $\eta(N)$ is determined by N and so are the $\tilde{K}_n$ values that are possible in the N-atom periodic cluster, while in the crystal orbital method for infinite crystals, the number of summands in Eq. (2) (order of interaction) is independent of the number of $\tilde{K}$ values used in constructing the operator $\hat{F}$. We have, therefore, two convergence problems in the latter method, while in the SPC they are reduced to one. Equation (8) is therefore solved for a given structure, as a function of $\eta(N)$, until convergence of the solutions is achieved. Another advantage of the self-consistent SPC approach, as compared to self-consistent methods that completely utilize the translational symmetry of the lattice, lies in the fact that the former method employs N'crystal one-electron states that are homogeneously distributed in the B.Z. (where $N'\sim 20$–30 is the number of unit cells) for recalculating the crystal potential in a given iteration, while in the latter method, only one to four states were usually considered,[14] and their choice from the complete B.Z. manifold is subjected to trial-and-error experiment.

Usually, one chooses the size N of the finite periodic cluster so that the eigenvalues $E_\lambda(\tilde{K}_n)$ reach the convergence limit at this $\eta(N)$ and that high symmetry $\tilde{K}_n$ points in the B.Z. (that are of interest in determining optical properties of the solid) will be included in the subset obtained. As previously demonstrated,[9] a two-dimensional finite periodic cluster of D_{3h} or D_{6h} point symmetry such as hexagonal BN and graphite, respectively, that is made up of 18 atoms ($\eta=2$) contains in its eigenvalue spectrum, among others, the Γ and P points in the B.Z. while the $N=32$ cluster ($\eta=3$) also contains the Q points. The values $E_\lambda(\tilde{K}_n)$ at these $\tilde{K}_n$ turn to be sufficient to determine a number of properties that are of interest regarding experimental optical data such as the work function, bandgap, the various bandwidths, and the band-to-band transition. The values of the one-electron energies $E_\lambda(\tilde{K}_n)$ and the atomic charges already reach the convergence limit at the interaction range of $\eta=3$. This requires a solution of a 128×128 secular determinant (Eq. 8) when four atomic orbitals are taken on each atom.

Since, in Expressions (7) and (8), we have not explicitly introduced translational periodicity, it is possible to treat by this method problems where perfect periodicity is lacking and $\tilde{K}_n$ is not a good quantum number. Such are the problems of point defects and the stability of the lattice against local displacements of a particular atom from its lattice site (this might be interesting when Frenkel pairs or lattice relaxations around a specific site or bond force-constants in the crystal are investigated). In this case, we do not analyze eigenvalues according to the $\tilde{K}_n$'s but still investigate the parentage of the defect levels in terms of those of the ideal lattice.

The calculations follow as in the perfect lattice case, except that a suitable row of the distance matrix $D_{pp'}^{(\eta)}$ is changed [and, accordingly, the $E_{pp'}^{(\eta)}(x)$, $E_{pp'}^{(\eta)}(y)$, and $E_{pp'}^{(\eta)}(z)$ matrices] when a local displacement of an atom is investigated or the chemical identity of one atom is altered, when impurities are investigated. Employment of charge-self-consistent methods for computing the clusters eigenvalues and atomic charges accounts for the charge redistribution introduced by the defect. Lattice relaxations around the defect are likewise easily introduced in the calculation. The calculation could be repeated at any desired interatom separation, thus providing a means of investigating crystal stability, cohesion, etc.

The matrix elements of Eq. (9) can be calculated in various levels of approximation. Owing to the complexity of *ab initio* computations, we adopted the semiempirical all-valence-electron methods that have been successful in accounting for a variety of molecular properties (such as geometries, electric dipole moments, nuclear spin coupling constant, ionization potentials, heat of formation, and atomic charges) for computing these matrix elements.

In our previous work, several of these approximations were examined on various electronic properties of boron nitride. In this work, we proceed with EXH (extended Huckel[26]) and IEXH (iterative extended Huckel[27]) approximations to the matrix elements, since these methods have proved to be the most successful.

The results for electronic properties of boron nitride as calculated using IEXH approximation, and for graphite as calculated by EXH approximation, were previously reported.[9] When we use the EXH approximation to evaluate the band structure of two-dimensional hexagonal boron nitride with a valence basis set ($2s$, $2p_x$, $2p_y$, and $2p_z$ orbitals per atom) without neglecting any overlap, Coulomb, and resonance matrix elements up to three orders of interaction, a band structure that is stable within less than 0.1 eV is obtained and the inhomogeneity of atomic charges on each sublattice (that is pronounced in the truncated-crystal type of calculation) is completely suppressed.

The full valence bandwidth is 19.1 eV (compared with 20 eV measured by soft x-ray photoelectron emission,[28]), the minimum of the lowest occupied band (the lowest Γ_1^+ point that is mainly of nitrogen $2s$ character) is obtained at $E_0+19.0$ eV (compared with the value measured by ESCA method relative to the Fermi energy $E_0+19.4$ eV),[29] and the $\pi\pi^*$ band-to-band transition energy at the Q_2 point in the B.Z. is calculated to be 6.29 eV (compared with the value of 6.5 eV as measured in dielectric experiments,[30] and with 6.2 eV as measured in reflectance[31]). The highest occupied valence band state comes out in this calculation as a σ state, and the highest π state falls 1.2 eV below, while other calculations on the perfect solid[12,32] reveal π character for the edge of the valence band. This behavior is also common to iterative extended Huckel and INDO (intermediate neglect of differential overlap) calculations on the same system[9] and was also previously observed to occur in similar calculations on the borazine molecule.[9,33] The bandgap thus obtained is 5.4 eV, while the direct $\pi\pi^*$ gap at P_1^- and P_2^- point is 6.6 eV (compared with the experimental values of 5.83 eV,[34] 5.4 eV,[35] and 3.6 eV[28]). The binding energy obtained in this calculation from the simple sum of the one-electron energies of the occupied bands is 6.0 eV (compared with the thermochemically measured value of 6.6 eV),[36] and the equilibrium atom-atom distance is calculated to be, under conditions of uniform stress, 1.44 Å (as compared with the crystallographic value of 1.446 Å).[37] The corresponding results for EXH cluster calculation on graphite were previously reported[9] and are in reasonable agreement with optical, crystallographic, and thermochemical experimental data.

The proposed calculation of point defect states in these lattices is a simple extension of the ideal crystal treatment. A vacancy or a substitutional impurity is placed in the periodic array of atoms and the new eigenvalue problem is solved again in the same LCAO frame. The defect site as well as every other atomic site will experience a "crystalline" environment extending out to 2–3 orders of neighbors, which is an interaction range sufficient to ensure reasonable convergence of the Hamiltonian matrix elements. Any inhomogeneity of charge distribution over each sublattice now reflects only the effects of the point defect, and the edges of the valence and conduction bands are properly defined with respect to the true band edges obtained in the ideal cluster calculation. The use of molecular orbital technique with atomic valence basis set enables calculation of the charge associated with each cluster orbital through standard population analysis.[38] Also, the fact that this model reasonably reproduces the ideal crystal equilibrium interatom distance when clusters without defects are considered (EXH formalism was shown[39,40] to perform favorably in this respect when the electronegativity difference between the atoms considered is not too high) suggests that it could be used to investigate model lattice relaxations around the defect site.

Calculations with the described model were performed on a nitrogen vacancy in hexagonal boron nitride, a vacancy in graphite and a boron impurity in graphite.

IV. NITROGEN VACANCY IN HEXAGONAL BORON NITRIDE

Nitrogen vacancy defects in hexagonal boron nitride were investigated by EPR[41–43] thermoluminescence[42,44] and thermally stimulated currents.[44] The tenfold splitting of the EPR signal of irradiated boron nitride was assigned by means of isotopic enrichment experiments[41] to a three-boron center created by an unpaired electron captured among three equidistant boron atoms with equal charge on them. The anisotropy of the g factor and the splitting has suggested that this electron is in a π type state.[41,43] The temperature dependence of these signals together with thermoluminescence and thermally-stimulated-currents measurements[44] reveal a thermal activation of this trapped electron into the conduction band. The energy difference between the defect state and the conduction state is 1.0 ± 0.1 eV. Photoluminescence experiments suggest that these centers quench the photo emission through nonradiative recombination.[42]

Figure 1 shows some high symmetry π levels of the ideal crystal calculated by the 32 periodic atom cluster without the defect (1a) and those after creating a nitrogen vacancy (1b) as a function of B–N distance. Since the calculated defect level is of π symmetry, only these states are shown, though the calculations were performed with the full $\pi+\sigma$ manifold, a need dictated by overlapping and charge redistribution effects between these bands.[9]

The highest occupied and lowest vacant ideal crystal π states (Fig. 1a) appearing at the P point and forming the edges of the π valence and conduction bands extend over the nitrogen and boron sublattices, respectively, and are pure $2p_z$ states due to symmetry requirements at the P point in the B. Z.[12] The lowest Γ state forms the bottom of the π valence band, while the Q state is the one exhibiting a Van Hove singularity in the joint density of states.[12] The number of free-atom states that collapse into each of these crystal states depends on the number of atoms in the periodic cluster, while the energies of these states are changed only very little by increasing the cluster from 18 to 32 atoms.

When a nitrogen vacancy is created (Fig. 1b), a new π level is split from the conduction band and appears in the forbidden gap (Fig. 1b, dashed line). The charge carried by this π level rests symmetrically on the three nearest neighbor boron atoms and on the second coordination shell of boron atoms. Such a center is capable of revealing a three-boron-center EPR signal. Analysis of the experimental anisotropic hyperfine splitting[41,43] using the free-atom value of $\langle r^{-3}\rangle$ for boron taken from atomic beam measurements[45] reveals that the square of the LCAO wavefunction coefficient on each neighboring boron site is 0.023. When this coefficient is computed with the free-atom Hartree–Fock value of $\langle r^{-3}\rangle$,[46] its value is 0.0187. This is to be compared with the calculated value of 0.017 obtained from the defect cluster orbital of 17 atoms and of 0.020 obtained from the 31 atom cluster. It should be mentioned, however, that the use of free-atom values of $\langle r^{-3}\rangle$ to analyze the experimental hyperfine splitting is only approximate, and actually the value appropriate for an atom carrying its real charge in the solid should be employed. This agreement suggests that the wavefunction in the defects' neighborhood is reasonably reproduced by this model.

The total electronic charge on the three neighboring boron atoms is increased upon creating a nitrogen vacancy, in both the π and σ manifolds, making the net

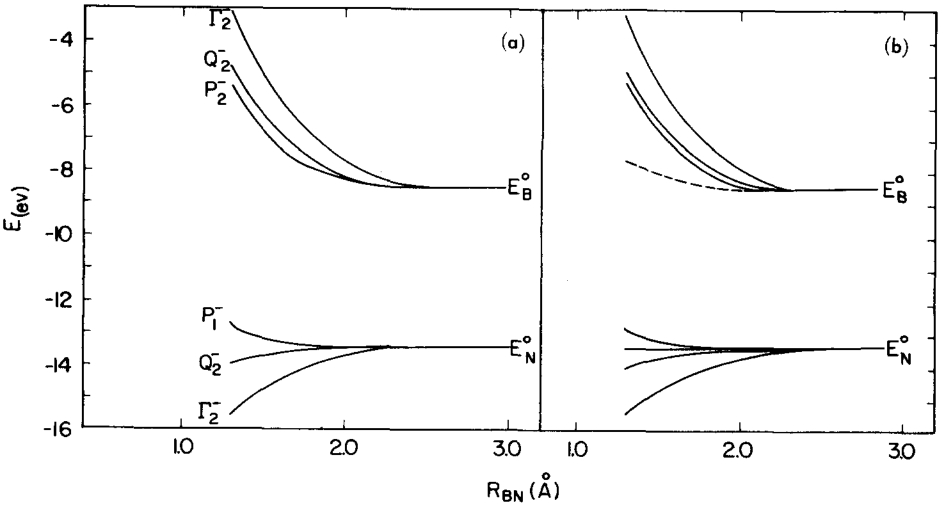

FIG. 1. One-electron energy levels of ideal (1a) and defect (1b) boron nitride clusters as calculated by EXH method.

atomic charge on these atoms less positive than that of a distant boron atom. Since such charge redistribution effects could not be adequately described by noniterative methods such as extended Huckel, this effect was calculated with a charge-self-consistent method. Applying the iterative extended Huckel LCAO method to the 18 and 17 atom clusters (for the experimental internuclear separation of 1.446 Å and with atomic orbital energies used in the previous paper)[9] reveals that the net atomic charge on each of the three boron atoms surrounding trigonally the vacant site decreases from its "normal" value of $+30e$ to $+0.26e$, the main effect being due to accumulation of π charge. This charge redistribution is due to the lack of the electronegativity effect of the central nitrogen atom in the vicinity of the three boron atoms. It should be mentioned that the π charge on a normal boron atom ($+0.50e$) is in accord with the value suggested by nuclear quadropole resonance experiments on hexagonal boron nitride[47] ($0.45e$). Similar experiments on damaged boron nitride have not yet been performed.

The gap between the defect orbital energy and the edge of the conduction band is 1.1 eV in this calculation, being close to the value obtained by simple extended Huckel method. The defect state is of a' symmetry (bonding between the three boron $2p_z$ orbitals) and therefore interacts with the conduction Γ_2^- state and the valence P_1^- state. The former crystal state undergoes a downwards shift, while the latter degenerate state extending over the nitrogen $2p_z$ sublattice is split in the presence of the defect. The P_2^- state extends only on the boron $2p_z$ sublattice and is therefore unaffected by removing a nitrogen atom. Owing to the interaction with the ideal crystal states, the defect charge distribution extends over a significant radius around the defect site. The close similarity between this charge distribution as obtained with the 17 and that with the 31 atom clusters indicates that 2–3 orders of neighbors are perhaps sufficient to describe this effect. On the other hand, a defect molecule treatment including only nearest neighbor orbitals[4] seems insufficient to account for the coupling of the defect with the crystal.

The energy difference between the defect state and the P_2^- bottom of the conduction state in the EXH approximation is 1.39 eV and 1.38 eV in the 17 and 31 atom clusters, respectively. [In the proposed method of calculating point defects, one obtains a superlattice, giving rise to a defect band. The small (~0.01 eV) difference between the defect energy levels of 17 and 31 atomic clusters indicates a very small dispersion of this band.] Since there are no experimental data to indicate the degree of relaxation of the lattice around the defect, we performed only model relaxations. An inward relaxation of 10% along the a' symmetry-adopted deformation direction[48] increases the gap between the defect state and the conduction edge to 1.51 eV, while an outward relaxation lowers this gap to 1.20 eV, the charge on the atoms remaining relatively unaffected by these changes. Temperature-dependent EPR measurements together with thermoluminescence and thermally-stimulated-currents data suggest a gap of 1.0 ± 0.1 eV[44] between the defect state and the conduction edge, a value that agrees favorably with the value predicted by the cluster calculation.

Calculations on a nitrogen vacancy employing open two-dimensional finite clusters, surrounded by hydrogens at the boundary,[9] reveal a nonmonotonic behavior of the energy of the defect state as a function of cluster size. This energy ranges between 0.94 eV for the $B_8N_7H_8$ cluster through 0.93 eV for the $B_{12}N_{11}H_{12}$ cluster to 1.1 eV for the $B_{14}N_{13}H_{14}$ cluster, when the same LCAO parameters are used. Inhomogenity of the charges over each sublattice introduces uncertainties both in the results for the ideal cluster and in the defect problem. These effects due to charge inhomogenity occur even in open clusters that are made up of identical atoms[6] and complicate considerably the interpretation of the results,[6,7,11] while the periodic cluster approach presented here is free of these limitations.

V. VACANCY IN GRAPHITE

Another familiar defect encountered in layered hexagonal structures is the isolated vacancy in graphite. Various workers have estimated the energy of its formation. The energy E_{vf} required to form such a vacancy is equal to $E_V - E_S$, where E_V is the energy required to remove an atom from its proper trigonal site to infinity, and E_S is the energy gained when this atom is attached to the surface (which in turn equals the experimental sublimation energy 7.44 eV).[49] Kanter[50] estimated E_{vf} to be 2.8 eV by measuring the activation energy of self-diffusion and using the experimental value of the sublimation energy and the calculated value for vacancy migration,[50,51] assuming that self-diffusion in graphite is due to vacancy migration. Baker and Kelly[52] were able to obtain the value of E_{vf} from observations on the formation of vacancy loops by quenching followed by annealing as 3.3 ∓ 0.9 eV. A much larger value (7.0 eV) was suggested by Hove[53] from specific heat measurements and also by Hennig from quenching experiments[54] ($\geqslant 6.6$ eV). Coulson *et al.*[4] have calculated E_{vf} using the experimental value of E_S and neglecting lattice relaxations and changes in hybridization around the vacant site. Their values are 10.74 eV or 13.05 eV, depending on the choice of empirical parameters. It was argued that rehybridization effects taking place around the vacant site could significantly lower these values, thereby decreasing the discrepancy between the theoretical values and the experimental results of Baker and Kelly[52] and Kanter.[50] Relaxations around the vacant site were not discussed, since their contribution to the activation energy is probably not very large, owing to the strong localization of the σ-bond structure.

The energy of vacancy formation was calculated with the periodic model neglecting relaxation effects and the small influence of the van der Waals interlayer interaction. Although periodic clusters of 18 and 32 atoms do not exactly reproduce the total one-electron energy per atom of the infinite cluster, since only a limited number of high symmetry one-electron states are included in its eigenvalue spectrum, previous calculation on the convergence of the total π one-electron energy as a function of cluster size[9] indicated that this property converges rapidly and is already very close to the convergence limit at the size of 18 to 32 atoms. The total $\pi+\sigma$ one-electron energy is supposed to converge similarly with cluster size. The calculations on the ideal cluster and on the cluster with a vacancy were performed with the iterative scheme IEXH, thereby allowing for self-consistent-charge redistribution and hybridization effects. The results for the ideal cluster of graphite were similar to those of the noniterative calculation, since the iteration procedure converges within one cycle (demanding a convergence criterion of $0.01\ e$ between successive iterations) owing to the homopolarity of the cluster and identical arrangements of atoms around each site. In this procedure, the hybridization state of each atom is not postulated but comes out of the charge-self-consistent treatment. The calculation of E_{vf} thus yields (taking the experimental value of E_S and the free atom parameters of the original work of Rein *et al.*)[15] values of 2.94 eV for the 17–18 atom cluster and 3.00 eV for the 31–32 atom cluster, which compare favorably with the experimental results of Kanter and with that of Baker and Kelly. The charge distribution over various atomic sites changes only slightly when a vacancy is created. The three carbon atoms surrounding the vacant site assume positive net atomic charge of $0.2\ e$, while the next nearest neighbors to the vacancy are only very slightly perturbed from their ideal cluster state. The vacancy itself could act as an electron trap that could capture a conduction electron. This is the usual picture adopted to explain transport and electron dynamics experiments of irradiated graphite. The charge transferred to the vacancy from its neighbors is mainly π charge, the trigonal σ frame being only slightly changed from its ideal cluster configuration. This is contrary to the behavior of the charge distribution around the three boron atoms surrounding trigonally a nitrogen vacancy in hexagonal boron nitride, where the electronic charge carried by these atoms is increased relative to a distant boron atom due to the lack of electron-withdrawing forces of a central electronegative nitrogen. This difference in behavior of an isolated vacancy in graphite and in boron nitride originates from the difference in electronegativity between the atoms in the unit cell in the latter case.

VI. SUBSTITUTIONAL BORON IMPURITY IN GRAPHITE

Another point defect particular to graphite is the boron impurity, which is the sole impurity element that has been shown to enter the carbon lattice substitutionally. Its behavior has been the subject of many experimental studies involving different properties.[55]

The substitutional boron impurity in graphite was treated in the periodic cluster approach by $C_{17}B$ models. The main features of this defect that were investigated are the charge distribution changes introduced by it, the bonding properties of a boron atom in a D_{3h} site, and the appearance of a defect orbital.

Upon introducing a boron atom in a trigonal site of the carbon periodic cluster, solving the new eigenvalue spectrum, and performing population analysis on the resulting wavefunctions, the carbon atoms surrounding the defect site are shown to transfer π charge to the boron and to pull a larger amount of σ charge away. The carbon atoms thus assume a negative net atomic charge ($-0.126e$ on the nearest neighbors to the boron and $-0.03e$ on the second shell), while the boron atom becomes positively charged, owing to its lower electronegativity relative to carbon. A neutral defect of this sort creates a positively charged acceptor that is capable of trapping conduction electrons.[55] Soule[56] suggested from the observed magnetic susceptibility curves of boron-doped graphite a 67% degree of ionization of the boron atoms (that are assumed to occupy substitutional sites) and a 75% degree of ionization from the measurement of hole carrier concentration in Hall experiments. The population analysis of the cluster wavefunctions in our model reveals a 56% ionization of an isolated boron impurity (at zero temperature), which compared reasonably with these results.

The $2p$ orbitals of the boron that are degenerate in the isolated atom split in the D_{3h} crystal field to a doubly degenerated in-plane orbital (forming a part of the σ manifold) and to a perpendicular π orbital. These states are shown to be stabilized relative to the free-atom levels and tend to delocalize over the first and second carbon atom shells surrounding the defect. A defect cluster orbital, which is singly occupied in the neutral cluster, is created upon introducing a substitutional boron atom. The wavefunction of this state is of π character and gets contributions from the central boron site and from the first and second shells of carbon atoms surrounding it. The charge carried by this state is distributed symmetrically on the three nearest and six next nearest carbon atoms. Such a defect should exhibit a four-line signal in the EPR hyperfine interaction due to the boron center, similar to the one-boron center observed in irradiated boron nitride[41] and to the boron center observed in irradiated crystals of BeO/B.[57] So far, EPR experiments on boron-doped graphite[58] have concentrated on the spin resonance due to the mobile charge carriers contributed by the skelton lattice and not by impurity states.

VII. SUMMARY

Small periodic clusters of hexagonally arranged atoms that have previously been shown to provide a good choice of molecular skeleton for calculating the electronic LCAO eigenvalues of ideal layered hexagonal solids via semiempirical quantum mechanical methods are used to calculate point defect states in these solids. The uniformity of charge on each sublattice of the ideal cluster and the possibility of investigating model relaxations and charge redistribution effects with all-valence electron quantum mechanical methods, achieved by this model, suggest that it could be used favorably for realistic defect problems.

[1] G. F. Koster and J. C. Slater, Phys. Rev. 95, 1167 (1954); 96, 1208 (1954).

[2] F. Bassani, G. Iadonisi, and B. Preziosi, Phys. Rev. 186, 735 (1969).

[3] K. H. Bennemann, Phys. Rev. A 137, 1497 (1965).

[4] C. A. Coulson, M. A. Herrnaes, M. Leal, E. Santos, and

S. Senent, Proc. R. Soc. Lond. A **274**, 461 (1963).
[5] B. S. Gourary and A. E. Fein, J. Appl. Phys. **33**, 331 (1962).
[6] R. P. Messmer and G. D. Watkins, Phys. Rev. B **7**, 2568 (1973); R. P. Messmer, Chem. Phys. Lett. **11**, 589 (1971).
[7] F. P. Larkins, J. Phys. Chem. Solids **4**, 3065, 3077 (1971).
[8] A. Zunger, J. Phys. Chem. Solids (to be published) (1974).
[9] A. Zunger, J. Phys. C **76**, 96 (1974).
[10] F. Bassani and G. P. Parravicini, Nuovo Cimento **50**, 95 (1967).
[11] C. A. Coulson and R. Taylor, Proc. Phys. Soc. Lond. A **65**, 815 (1952).
[12] E. Doni and G. P. Parravicini, Nuovo Cimento A **63**, 117 (1969).
[13] R. Taylor and C. A. Coulson, Proc. Phys. Soc. Lond. A **65**, 834 (1972).
[14] D. J. Stukel, R. N. Euwema, and T. C. Collins, Phys. Rev. **179**, 740 (1969).
[15] W. E. Rudge, Phys. Rev. **181**, 1024 (1969); **181**, 1033 (1969).
[16] D. Brust, Solid State Commun. **9**, 481 (1971).
[17] F. Herman, R. L. Kuglin, C. D. Kuglin, J. P. Van Dyke, and S. Skillman, Methods Comput. Phys. **8**, 193 (1968).
[18] L. F. Mattheiss, J. H. Wood, and A. C. Switendick, Methods Comput. Phys. **8**, 110 (1968).
[19] G. Del Re, J. Ladik, and G. Biczo, Phys. Rev. **155**, 997 (1967).
[20] J. M. Andre, J. Chem. Phys. **50**, 1536 (1969).
[21] A. Imamura, J. Chem. Phys. **52**, 3168 (1970).
[22] K. Morakuma, J. Chem. Phys. **54**, 962 (1971).
[23] S. O'Shea and D. P. Santry, J. Chem. Phys. **54**, 2667 (1971).
[24] D. L. Beveridge and I. Jano, J. Chem. Phys. **56**, 4744 (1972).
[25] S. G. Davidson and J. D. Levine, Solid State Phys. **25**, 1 (1970).
[26] R. Hoffman, J. Chem. Phys. **39**, 1392 (1963); **40**, 2474 (1964).
[27] R. Rein, H. Fukuda, H. Win, and G. A. Clark, J. Chem. Phys. **45**, 4743 (1966).
[28] V. A. Formichev, Sov. Phys.-Solid State **13**, 754 (1971).
[29] K. Hamrin, G. Johansson, U. Gelius, C. Nordling, and K. Sigbahan, Phys. Scr. **1**, 277 (1970).
[30] R. Vilanov, C. R. Acad. Sci. B **272**, 1066 (1971).
[31] W. J. Choyke (unpublished data).
[32] J. Zupan, Phys. Rev. B **6**, 2477 (1972).
[33] P. M. Kuznesof and D. F. Shriver, J. Am. Chem. Soc. **90**, 1683 (1960).
[34] W. Baronian, Mater. Res. Bull. **7**, 119 (1972).
[35] S. Larach and R. E. Shrader, Phys. Rev. **104**, 68 (1956).
[36] *JANAF International Tables* (Dow Chemical, Midland, Michigan, 1965).
[37] R. S. Pease, Acta Crystallogr. **5**, 356 (1952).
[38] R. S. Mulliken, J. Chem. Phys. **23**, 433 (1955).
[39] G. Blyholder and C. A. Coulson, Theor. Chim. Acta **10**, 316 (1968).
[40] L. C. Allen and J. D. Russel, J. Chem. Phys. **46**, 1029 (1967).
[41] G. Romelt, Proc. Int. Symp. Lattice Defects Tokyo, 407 (1966).
[42] M. B. Khusidman and V. S. Neshpor Fiz. Tverd. Tela **10**, 1229 (1968) [Sov. Phys.-Solid State **10**, 975 (1968)]; Poroshk. Metall. **8**, 72 (1970).
[43] A. W. Moore and L. S. Singer, J. Phys. Chem. Solids **33**, 343 (1972).
[44] A. Katzir, J. T. Suss, and A. Halprin, Phys. Lett. A **41**, 117 (1972).
[45] G. Wessel, Phys. Rev. **92**, 1581 (1953).
[46] C. M. Hurd and P. Coodin, J. Phys. Chem. Solids **28**, 573 (1967).
[47] A. H. Silver and P. J. Bray, J. Chem. Phys. **32**, 288 (1960).
[48] A. Sussman, Proc. Phys. Soc. Lond. **79**, 758 (1962).
[49] H. T. Knight and J. P. Rink, J. Chem. Phys. **29**, 449 (1958).
[50] D. M. Kanter, J. Chem. Educ. **33**, 272 (1956).
[51] G. J. Dienes, J. Appl. Phys. **23**, 1194 (1952).
[52] C. Baker and A. Kelly, Nature (Lond.) **193**, 235 (1962).
[53] J. E. Hove, *Industrial Carbon and Graphite* (Soc. Chem. Ind., London, 1958), p. 501.
[54] G. R. Hennig, Appl. Phys. Lett. **1**, 55 (1962).
[55] A. Marchand, in *Chemistry and Physics of Carbon*, edited by P. L. Walker (Marcel Dekker, New York, 1971), Vol. 7, p. 155.
[56] D. E. Soule, *Proceedings of the 5th Carbon Conference*, Universit Park, PA, 1962 (Pergamon, London, 1962), Vol. 1, p. 13.
[57] A. R. Reinberg, J. Chem. Phys. **41**, 850 (1964).
[58] G. Wagoner, private communication to J. W. McClure and Y. Yafet, cited in Ref. 56, Vol. 1, p. 22.